0.75–1.1-THz Waveguide-Integrated Amplitude Modulator based on InAs photo-excitation

J. Guise[1], H. Ratovo[1], M. Thual[2], J. Hesler[3], T. Reck[3], E. Centeno[4], J.B. Rodriguez[1], L. Cerutti[1], F. Gonzalez-Posada[1], T. Taliercio[1], and S. Blin[1]
[1]IES, Univ Montpellier, CNRS, Montpellier, France
[2]Institut FOTON, Univ Rennes, CNRS, Lannion, France
[3]VDI Inc., 979 Second street, S.E. Suite 309, Charlottesville, VA 22902-6172, USA
[4]Institut Pascal, Univ Clermont-Auvergne, CNRS, Aubière, France

***Abstract*—We present an integrated amplitude modulator operating in the 0.750–1.1-THz frequency range. This component offers typically a modulation depth of 10 dB, a modulation bandwidth of 40 MHz and insertion losses of 6 dB. The modulator is based on the optical pumping of an InAs layer deposited on a semiconductor substrate, using moderate pumping optical power of less than 600 mW at a wavelength of 1 µm. Such performances are possible thanks to its integration within a WR1.0 waveguide.**

I. INTRODUCTION

THz waves are attractive for many applications [1] involving imaging and/or spectroscopy (industrial process controls, security, biology, medicine, etc.) and in high-date-rate communications. However, there is still active research on components at these frequencies, mainly on THz sources, detectors, but also on key components such as THz modulators. Metamaterials are good candidates to efficiently manipulate THz waves, and have been demonstrated to modulate THz using electrical [2,3], mechanical [2,4] or optical [5,6,7] stimuli. We recently proposed an original THz modulator based on the photo-excitation of an InAs semiconductor [8] that was an interesting compromise in terms of required optical pump power and modulation bandwidth in comparison to reported optically-pumped modulators using materials such as GaAs [6] or Si [7]. Additionally, we conducted Comsol simulations of a modulator based on a InAs slab grown on a GaAs substrate, that is integrated within a standard WR1.0 waveguide [9]. Integration presents an obvious practical interest for end-user, but it also allows to increase the optical pump intensity (for constant power) thus improving the performance of the modulator, since the modulation depth depends on the photo-generated free-carrier density that scales with optical intensity. Here, we will present the experimental characterization of the integrated modulator.

II. AMPLITUDE MODULATOR INTEGRATION

A photo of the modulator is presented in Fig. 1. An incoming THz signal, generated using a frequency-multiplier chain (VDI, Inc.) was focused thanks to Teflon lenses on the modulator. The signal was collected using a standard diagonal horn antenna whose WR1.0 output waveguide could be connected to our integrated modulator. The semiconductor was placed in sandwich between the horn antenna and a commercial waveguide. This commercial waveguide was mechanically processed to bring an optical fiber close the semiconductor, the InAs layer facing the optical fiber output at the optical Brewster angle to improve the optical pumping efficiency. We used a home-made integrated micro-lensed fibre [10] to optimize the overlap between the optical beam and the THz transverse mode within the waveguide. In fine, the incoming THz signal was transmitted through an optically-excited semiconductor, thus allowing for optically-driven amplitude modulation. The output signal was measured thanks to a calibrated heterodyne receiver allowing for spectrum measurements.

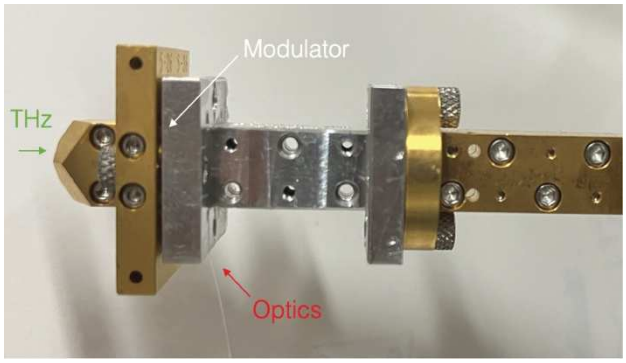

Fig. 1. Photo of the integrated modulator at receiver side. The incoming THz signal is collected thanks to a standard diagonal horn antenna with a WR1.0 output waveguide. The semiconductor structure is placed between this output and a standard WR1.0 waveguide (silver component). Mechanical process on this waveguide allows to bring an optical fiber close to the semiconductor for optical pumping. The modulator was then connected to a THz receiver for measurements (right gold component on the photo).

Previous work showed that 1.55-µm optical excitation was possible [9], and attractive as it corresponds to telecommunication wavelengths thus offering a large variety of on-shelf low-cost fiber-optic components. Here, we used a 1 µm excitation wavelength for practical reasons, namely to take advantage of an available polarization-maintaining fiber-optic amplifier. Therefore, since the photon flux scales with wavelength, the optical pumping efficiency is reduced by about 30% but this drop of efficiency can be easily compensated by an increased optical power thanks to the optical amplifier.

III. EXPERIMENTAL CHARACTERIZATION

We conducted static and dynamic THz characterizations of the amplitude modulator, to evaluate the insertion losses, the modulation depth and the modulation bandwidth.

As static characterizations are concerned, we measured insertion losses of about 6 dB. These insertion losses are mainly due to the residual absorption of the 5-µm-thick InAs layer, a thinner layer would offer lower insertion losses, but a reduced modulation depth. We evaluated by simulations the losses due to the spacing of about 500 µm (semiconductor thickness) between the two waveguides, and the losses due to the hole within the waveguide to place the optical fiber, but these are

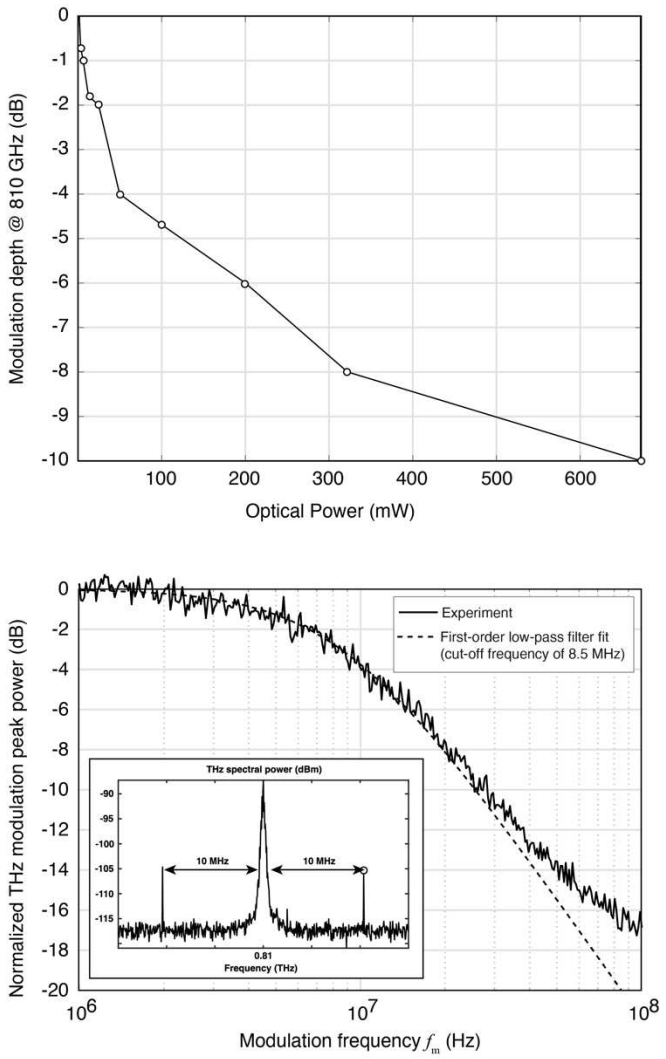

Fig. 2. Experimental characterization of the THz modulator.
The top figure shows the modulation depth as a function of the optical pump power at 1 µm. Additional insertion losses of about 6 dB have to be considered to evaluate overall transmission.
The bottom figure shows how the modulation depth degrades with modulation frequency for a sinusoidal excitation, showing a transfer function close to a single-order low-pass filter. The inset shows the typical spectrum of the modulated signal at detection, the amplitude of the modulation peak (here for a modulation at a frequency of 10 MHz) is then reported on the transfer function for each modulation frequency.

negligeable. Figure 2 (top) shows how transmission drops with optical power, we observe a modulation depth close to 10 dB for an optical power of 600 mW. Again, such a modulation depth could be increased using either a thicker InAs layer, an increased optical power, or an increased optical wavelength (as long as it remains below the bandgap wavelength).

In terms of dynamic characterizations, we modulated the optical amplitude thanks to a Mach-Zehnder amplitude modulator. A sinusoidal signal was used for modulation, therefore, as shown in the inset of Fig 2 (bottom), two modulation lines appear in the THz spectrum at the output of the modulator, at frequencies symmetrically offsetted from the carrier frequency by the modulation frequency. We measured the amplitude of one of these modulation lines as a function of modulation frequency, to evaluate the dynamic transfer function of the THz amplitude modulator. As shown in Fig. 2 (bottom), this transfer function corresponds to a first-order low-pass filter whose cut-off frequency mainly depends on the lifetime of photo-generated carriers in the InAs layer. This lifetime presents different contributions related to the material (Shockley–Read–Hall lifetime, Radiative lifetime, Auger lifetime) and the possible recombination at interface with the substrate. In comparison to the InAs slab that offered a 2-MHz cut-off frequency [8], this configuration of a InAs layer grown on a GaAs substrate offers an increased bandwidth of 8.5 MHz.

IV. Summary

We presented a functional amplitude modulator with attractive performances that could be directly integrated in WR1.0 waveguided THz systems, operating at frequencies of 0.75–1.1 GHz. The modulation bandwidth of this modulator offers possible application that requires lock-in detection, e.g. for imaging or spectroscopy measurements. Further work consists in the study of alternative materials to propose functional modulators at any other THz frequency.

Acknowledgments

This work was supported in part by Région Occitanie/Pyrénées-Méditerranée (HERMES platform) and in part by the European Regional Development Fund (FEDER). This work was also supported by ANR under the *"*Investment for the Future" programs (MUSE STAE ANR-16-IDEX-0006, EquipEx EXTRA ANR-11-EQPX-0016*)* and under the SPATIOTERA program (grant number ANR-19-CE24).

References

[1] Y. Huang et al., "From Terahertz Imaging to Terahertz Wireless Communications," *Engineering*, in press, 2022.
https://doi.org/10.1016/j.eng.2022.06.023
[2] M. Rahmani et al., "Reversible thermal tuning of all-dielectric metasurfaces," *Advanced Functional Materials,* vol. 27, no. 31, p.1700580, 2017.
https://doi.org/10.1002/adfm.201700580
[3] J.-Y.Wu, et al., "Active metasurfaces for manipulatable terahertz technology," *Chinese Physics B*, vol. 29, p. 94202, Sept. 2020.
https://doi.org/10.1088/1674-1056/aba613
[4] R. Degl'Innocenti et al., "All-integrated terahertz modulators," *Nanophotonics*, vol. 7, pp. 127–144, Jan. 2018.
https://doi.org/10.1515/nanoph-2017-0040
[5] Q.-Y. Wen et al. "Graphene based All-Optical Spatial Terahertz Modulator," *Scientific Reports*, vol. 4, pp. 1–5, Dec. 2014.
https://doi.org/10.1038/srep07409
[6] Y. Yang et al., "Transient GaAs Plasmonic Metasurfaces at Terahertz Frequencies," *ACS Photonics*, vol. 4, no 1, p. 15-21, janv. 2017.
https://doi.org/10.1021/acsphotonics.6b00735
[7] Z. Jiang et al., "Investigation and Demonstration of a WR-4.3 Optically Controlled Waveguide Attenuator," in *IEEE Transactions on Terahertz Science and Technology*, vol. 7, no. 1, pp. 20-26, Jan. 2017.
https://doi.org/10.1109/TTHZ.2016.2635443
[8] E. Alvear-Cabezón et al., "Epsilon near-zero all-optical terahertz modulator", *Applied Physics Letters*, vol. 117, no 11, p. 111101, sept. 2020.
https://doi.org/10.1063/5.0012206
[9] J. Guise et al., "Waveguide-integrated optically-tuned THz modulator," *IRMMW conference,* 2022.
https://doi.org/10.1109/IRMMW-THz50927.2022.9895784
[10] M. Thual et al, "Contribution to research on Micro-Lensed Fibers for Modes Coupling", *Fiber and Integrated Optics*, vol. 27, no. 6, 2008.
https://doi.org/10.1080/01468030802272450